

Prediction of tribological performance of AA8011/wt.%ZrO₂ based composites fabricated by stir casting route

Proc IMechE Part E:
J Process Mechanical Engineering
2022, Vol. 236(6) 2420–2433
© IMechE 2022
Article reuse guidelines:
sagepub.com/journals-permissions
DOI: 10.1177/09544089221096096
journals.sagepub.com/home/pie



Vinoth B.¹, Alagarsamy S.V.^{2*} , Meignanamoorthy M.³
and Ravichandran M.^{4,5}

Abstract

Aluminium alloy composites are most popular owing to their versatile applications like high performance parts in aerospace, automotive and marine industries. The intent of current research work is, to predict the optimal parameters for dry sliding wear behaviour of AA8011 matrix composites by using multi attribute decision making method. The varying proportions of zirconia (ZrO₂) particles filled composites such as AA8011-5 wt.% ZrO₂, AA8011-10 wt.% ZrO₂ and AA8011-15 wt.% ZrO₂ were synthesized through stir casting method. The microstructure of the proposed composites taken by scanning electron microscopy (SEM), and it was ensure the presence of reinforcement particles homogeneously distributed within the matrix alloy. The produced composites were subjected to conduct the dry sliding wear test by using pin-on-disc test rig. During the experiments, four wear control parameters with three levels namely, reinforcement (5 wt.%, 10 wt.% and 15 wt.%), applied load (9.81 N, 19.62 N and 29.43 N), sliding velocity (0.94 m/s, 1.88 m/s and 3.76 m/s) and sliding distance (1000 m, 1500 m and 2000 m) were used. A Taguchi coupled TOPSIS method was employed to predict the multiple responses such as wear rate (WR) and coefficient of friction (COF) of produced composites. Experimental result has been observed that, the reinforcement content was the most remarkable parameter on WR and COF with contribution of 55.06%, subsequently by applied load and sliding velocity with contribution of 26.32% and 12.84% respectively. The worn out surfaces of the tested composite was investigated through SEM analysis.

Keywords

AA8011, ZrO₂, stir casting, wear parameters, Taguchi method, TOPSIS

Date received: 25 June 2021; accepted: 19 March 2022

Introduction

In recent decades, Al alloys are most preferable materials in high tech engineering applications like defence, aerospace and automotive sectors owing to their excellent strength-to-weight ratio, damping capacity and better thermal related properties.¹ It is particularly applied in the production of high performance parts such as cylinder block, piston, connecting rod, driven shafts and brake disc which can be pretentious by higher and cyclic stresses.² In general, Al alloys exhibit poor tribological characteristics which leading to evils in confrontational conditions. In order to enhance the tribological properties, these alloys are integrated with hard or self lubricating ceramic particulates such as SiC, TiC, Al₂O₃, TiO₂, B₄C, ZrO₂, Si₃N₄ and Gr, etc.^{3–10} Therefore, extensive research has been made on the development of those composites, which may give the appreciable wear resistance. In terms of inexpensive and ease of fabrication, the development of Aluminium Matrix Composites (AMCs) are gaining more importance. Furthermore, the properties of AMCs are drastically affected by the fabrication method. In recent era, many researchers employed different kinds of fabrication techniques such as

stir casting, powder metallurgy, infiltration and spray deposition etc.¹¹ In these techniques, stir casting is a potential candidate to eradicate the defects like porosity, crack and tears. In addition to that, it has very simple, cost effective and to makes good contact in between matrix and reinforcement due to stirring action.¹² Karthikeyanand Jinu¹³ analyzed

¹Department of Mechanical Engineering, Mangayarkarasi College of Engineering, Madurai-625 402, Tamil Nadu, India

²Department of Mechanical Engineering, Mahath Amma Institute of Engineering and Technology, Pudukkottai-622 101, Tamil Nadu, India

³Department of Mechanical Engineering, K. Ramakrishnan College of Engineering, Tiruchirappalli-621 112, Tamil Nadu, India.

⁴Department of Mechanical Engineering, K. Ramakrishnan College of Engineering, Tiruchirappalli-621 112, Tamil Nadu, India.

⁵Department of Mechanical Engineering and University Centre for Research & Development, Chandigarh University, Mohali-140 413, Punjab, India

Corresponding author:

Alagarsamy S.V., Department of Mechanical Engineering, Mahath Amma Institute of Engineering and Technology, Pudukkottai-622 101, Tamil Nadu, India.
Email: s.alagarsamy88@gmail.com

the properties and microstructure of ZrO₂ filled LM25 alloy composites produced by stir casting route and the SEM morphology evident the homogeneous distribution of filler content with Al alloy due to proper selection of casting parameters. Bai-Xin Dong et al.¹⁴ investigated the microstructure and mechanical properties of TiB₂ inclusion of Al-Si based composites. They observed that the addition of TiB₂ particles can significantly manipulate the microstructure and also exhibit good interfacial bonding, thus enhance the strength and elongation of the proposed composites. Madhusudhan et al.¹⁵ developed the AA7068 matrix composites via stir casting method by adding different wt.% of ZrO₂ particles and noticed the uniform dispersion of particles enhanced the hardness and tensile strength. Hong-Yu Yang et al.¹⁶ studied the interface formation and bonding behaviour of (TiC + TiB₂)/Al composites. They noticed that the yield strength, compressive strength and plastic strain drastically improved when addition of 60 vol % (TiC + TiB₂) particles into Al composites. This can be attributed to the improvement in interfacial bonding strength and therefore the increase in the energy dissipation of crack propagation. Zhu et al.¹⁷ observed that the wear resistance of composites improved when an inclusion of ZrO₂ content and also its found the less friction coefficient produced. Pandiyarajan et al.¹⁸ analyzed the effect of ZrO₂ and graphite content on tribological behaviour of AA6061 matrix composites synthesized via stir casting route. They have noticed that the addition of ZrO₂ content reduces the wear because its act as a resistant. There are several variables that have a major effect on composite wear behaviour, such as filler content, load, disc velocity, sliding distance and counter disc material properties etc.¹⁹ To determine the optimum range of factors for obtain less WR, the various optimization techniques are employed. Alagarsamy and Ravichandran²⁰ optimized the control variables on WR of TiO₂ reinforced AMCs by using Taguchi method and reported that the less WR is obtained at a load of 9.81 N with a velocity of 2.82 m s⁻¹ and a sliding distance of 1000 m. Neeraj Kumar et al.²¹ studied the wear behaviour of B₄C incorporated Al-Mg-Si composites and observed that the WR increases with increase in sliding distance. However, the inclusion of B₄C particles decreasing the WR due to enhanced the surface hardness. Ayyanar et al.²² presented the tribological characteristics of AA6061/B₄C/h-BN composites and reported that the addition of solid lubrication h-BN particles brings the low WR and friction due to formation of tribo-layer on the worn surfaces shown in SEM morphology. Ghandvar et al.²³ reported the wear behaviour of A356-ZrO₂ composites under dry sliding conditions and they have noted that wear loss linearly increases with increase in sliding distance, while an increase in applied load increasing the COF. Sathishkumar et al.²⁴ conducted the wear test on AA8011 hybrid composites by using pin on disc tribometer and its understood that the high WR and COF produced at maximum load with higher sliding distance conditions. Mukesh Kumar²⁵ have developed AA356-Al₂O₃/SiC/Gr alloy composites via semi

automatic stir casting method and studied the effects of sliding wear parameters like sliding velocity, sliding distance and load. It was revealed that normal load was the primary significant factor trailed by sliding velocity. Magibalan et al.²⁶ have optimized the wear parameters namely load, time and sliding velocity using TOPSIS method to reduce the WR and COF of the fabricated composite.

From the comprehensive literatures we had observed that the prediction of tribological behaviour of AMCs is a difficult phenomenon, since it is dependent on several variables such as reinforcement content, load, sliding velocity and sliding distance. Hence, in order to predict the optimum tribological behaviour of AMCs, the statistical scientific assessment is very important. Furthermore, the detailed literatures revealed that there is no experimental and statistical work is directed towards the study of tribological behaviour of AA8011-ZrO₂ composites developed through stir casting technique. Hence, the aim of the present work was employed to predict the tribological behaviour of ZrO₂ particles reinforced AA8011 based composites produced via stir casting route. A pin-on-disc tribometer was used to conduct the tests by chosen various factors with different conditions. A Taguchi technique combined with TOPSIS approach was applied to find out the optimum range of parameter conditions on the tribological behaviour of the proposed composites.

Experimental details

Matrix and reinforcement

For the fabrication of composites, AA8011 matrix metal (*Metal Mart, Coimbatore, India*) and ZrO₂ reinforcement (*LOBA Chemie, Mumbai, India, 99.5% purity*) with an average particle size of 10 µm were taken respectively. The chemical constituents of the aforesaid alloy contain (wt.%) Fe-0.6, Si-0.5, Mn-0.20, Cu-0.10, Zn-0.10, Ti-0.08, Mg-0.05, Cr-0.05 and Al-remaining. By adopting the liquid state method like stir casting route, three different proportions (5 wt.%, 10 wt.% and 15 wt.%) of ZrO₂ particles were dispersed in the AA8011 matrix to get the experimental composites specimen.

Fabrication of composites

In the current investigation, stir casting method was employed for the fabrication of composites due to the indispensable merit of homogeneity distribution of reinforcement particles in Al matrix by means of mechanical stirring. At first, the weighted amount of AA8011 ingots were kept into the graphite crucible of the electrical resistance furnace and the furnace temperature was maintained at 750 °C, till whole alloy was completely melted. On the other side, the ZrO₂ particles at 5 wt.%, 10 wt.% and 15 wt.% were preheated for 1 h at a temperature of 300 °C to eradicate the moisture content and to promote the wettability with the molten Al alloy. Concurrently, the mechanical stirring has been initiated by immersing

the three-blade stainless steel stirrer into the molten alloy thus creates vortex in the melt. Then, the heat treated ZrO₂ particles were incessantly injected into the vortex of Al molten slurry. Meanwhile, the stirring speed was increased at 300 rpm and it was maintained for 10 min. Thereafter, the mixed composite slurry was poured into the preheated mould and allowed to solidify in air to normal room temperature. After solidification, the composite specimens detached from the mould and desired shape was produced using suitable machining process. Figure 1 shows the SEM images of the fabricated AA8011-ZrO₂ composites which was taken by a scanning electron microscopy (Vega3, Tescan, Czech Republic). Figures 1(a) and (b) reveals the SEM micrographs of AA8011-10 wt.% ZrO₂ and AA8011-15 wt.% ZrO₂ composites, respectively. The absence of clusters or agglomerations of ZrO₂ particles can clearly be seen in both figures, and also it showing a uniform dispersion of ZrO₂ particles inside the AA8011 matrix. This can be attributed to the optimized stir casting parameters used to fabricate the composites.

Dry sliding wear test

A TR-20 DUCOM pin-on-disc tribometer was used to conduct the dry sliding wear tests as per ASTM G-99 standard. This tribometer consists of a counterpart disc made of EN-31 hardened steel having a hardness of 60 HRC. The essential dry sliding wear control parameters were chosen from the available literatures and are varied in three levels as depicted in Table 1.²⁷ A typical Taguchi L₂₇ orthogonal array was chosen to perform the experiments, as seen in Table 2, to minimize the number of experiments for the selected parameters and their levels. The wear sample pins measuring 10 mm × 10 mm × 30 mm were prepared from the as-casted AA8011-ZrO₂ composites. During the wear test, the composite pin was pressed to slide over the rotating counter disc without lubrication condition thus produces sliding wear as the sample pin adheres to it. The composite pin and disc were treated with acetone solution before and after the experimental run and also polished using emery sheet to achieve clean surface contact between them. Based on the mass loss of pins, the volumetric wear rate was computed. By using an electronic precision balance machine, the initial and final mass of the composite pin was weighted. For each experimental run, the standard formula for WR and COF as used elsewhere,²⁸ and given in Table 2.

Methodologies and implementation

Taguchi technique

Taguchi technique can be used to predict the responses through a proper setting of design parameters and also diminish the data integrity response to the source of attribute.²⁹ This technique is a powerful method for controlled data acquisition and analysis of the impact of process

parameters to a particular response, which is an unspecified measure of these process variables. This approach is based on orthogonal arrays and ANOVA to reduce the number of tests and to efficiently increase product consistency.³⁰ During this investigation, to predict the WR and COF for the produced composites under dry sliding condition by using the various control parameters. In Taguchi method, three objective of S/N ratio are used to predict the response. The goal of current study is, to obtain the minimum WR and COF, hence smaller-the-better S/N ratio was chosen and the equation (1) was applied.

$$S/N \text{ ratio} = -10 \log_{10} (1/n) \sum_{k=1}^n Y_{ij}^2 \quad (1)$$

Where n – no. of trials, Y_{ij} – measured response where $i = 1, 2, 3, \dots, n; j = 1, 2, 3, \dots, k$. The calculated S/N ratio are depicted in Table 2.

TOPSIS method

TOPSIS method was introduced by Hwang and Yoon, in which main aspect is to indicate the best alternatives having shortest distance from the positive ideal solution and farthest from the negative ideal solution.³¹ The positive ideal solution is a solution that tries to maximize the profit criteria and minimizes the cost criteria, whereas negative ideal solution maximizes the cost criteria and minimizes the profit criteria. The given steps are employed by TOPSIS method for the selection of best alternative from among these available alternatives is as follows,

Step 1: Construct the normalized decision matrix (r_{ij}). During this step, the responses are normalized in the range of 0 to 1 by using equation (2),

$$r_{ij} = x_{ij} / \sqrt{\sum_{i=1}^m x_{ij}^2} \text{ for } i = 1, 2, \dots, m \text{ and } j = 1, 2, \dots, n. \quad (2)$$

Step 2: Construct the weighted normalized decision matrix (v_{ij}) by using equation (3). By multiplying the normalized decision matrix with its assigned weights (w_j). In this study, we assigned equal weights ($w_j = 0.5$) due to both responses are equally important.

$$v_{ij} = r_{ij} \times w_j \text{ for } i = 1, 2, \dots, m \text{ and } j = 1, 2, \dots, n. \quad (3)$$

Where, w_j is the weight of the j^{th} attribute and $\sum_{j=1}^n w_j = 0.5$. The estimated normalized decision matrix and weight matrix are provided in Table 3.

Step 3: In this step the ideal positive (V_j^+) and ideal negative (V_j^-) alternative of the responses are obtained

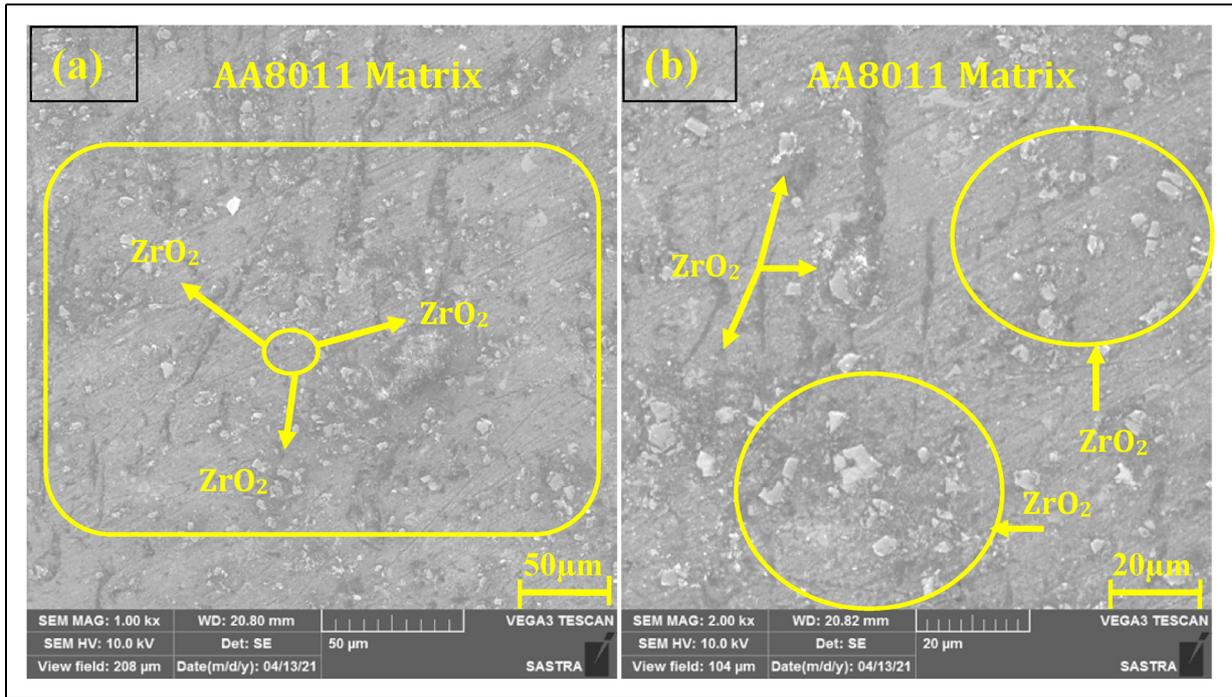


Figure 1. Microstructure of produced AA8011-ZrO₂ composites.

Table 1. Control parameters with its level.

Symbol	Control parameters	Unit	Level		
			1	2	3
A	Reinforcement	wt.%	5	10	15
B	Applied load	N	9.81	19.62	29.43
C	Sliding velocity	m/s	0.94	1.88	3.76
D	Sliding distance	m	1000	1500	2000

by using equations (4) & (5).

$$V_j^+ = \left\{ \sum_{i=1}^{\max} V_{ij}/j \in J, \sum_{i=1}^{\min} V_{ij}/j \in J^l \right\} \quad (4)$$

$$V_j^- = \left\{ \sum_{i=1}^{\min} V_{ij}/j \in J, \sum_{i=1}^{\max} V_{ij}/j \in J^l \right\} \quad (5)$$

Where, J is associated with the profit parameters and J^l is associated with non-profit parameters. The positive and negative ideal solutions of the responses are provided in Table 4.

Step 4: This step is to obtain the separation measures of each alternative from the positive and the negative ideal solution is evaluated by Euclidean distance using the equation (6) & (7) and results are depicted in Table 7.

$$S_i^+ = \sqrt{\sum_{j=1}^n (v_{ij} - v_j^+)^2}, j = 1, 2, \dots, m \quad (6)$$

$$S_i^- = \sqrt{\sum_{j=1}^n (v_{ij} - v_j^-)^2}, j = 1, 2, \dots, m \quad (7)$$

Step 5: At last, the relative closeness (RC) of each alternative to the ideal solution is computed by using equation (8) and the results are given in Table 5.

$$RC_i^+ = \frac{S_i^-}{S_i^+ + S_i^-} \quad (8)$$

RC value represents a single response by converting the multiple responses (i.e. WR and COF) into a single response. The best response was identified according to preference rank of higher RC value is shown in Figure 2. From the Fig, it clearly indicates the RC values of each 27 experimental run. Among the values of 27 RC, experiment no. 19 showed the best multiple response characteristics because it represents the higher RC value (0.92768). Hence, the experiment no. 19 yield the optimum parameters level for obtain the minimum WR and COF of the fabricated AA8011-ZrO₂ composites during dry sliding process.

Results and discussion

Effect of control parameters on Wr

Figure 3 graphically depict the effect of various control parameters on the WR during dry sliding wear for the fabricated composites. From the graph, it can be reveal that reinforcement content has a primary influencing factor on WR,

Table 2. Experimental layout using L27 (3^4) orthogonal array.

Ex. No	Input parameters				Output response		S/N ratio	
	Reinforcement (wt.%)	Applied load (N)	Sliding velocity (m/s)	Sliding distance (m)	WR (mm^3/m)	COF	WR (dB)	COF (dB)
1	5	9.81	0.94	1000	0.00441	0.564	47.1112	4.97442
2	5	9.81	1.88	1500	0.00515	0.696	45.7723	3.14782
3	5	9.81	3.76	2000	0.00579	0.864	44.7464	1.26973
4	5	19.62	0.94	1500	0.00477	0.588	46.4296	4.61245
5	5	19.62	1.88	2000	0.00551	0.744	45.1849	2.56854
6	5	19.62	3.76	1000	0.00662	0.912	43.5894	0.80010
7	5	29.43	0.94	2000	0.00771	0.636	42.2589	3.93086
8	5	29.43	1.88	1000	0.00716	0.792	42.9078	2.02550
9	5	29.43	3.76	1500	0.00698	0.936	43.1291	0.57448
10	10	9.81	0.94	1500	0.00399	0.384	47.9805	8.31338
11	10	9.81	1.88	2000	0.00464	0.492	46.6790	6.16070
12	10	9.81	3.76	1000	0.00381	0.576	48.3815	4.79155
13	10	19.62	0.94	2000	0.00491	0.504	46.1872	5.95139
14	10	19.62	1.88	1000	0.00473	0.636	46.5120	3.93086
15	10	19.62	3.76	1500	0.00435	0.720	47.2302	2.85335
16	10	29.43	0.94	1000	0.00521	0.504	45.6716	5.95139
17	10	29.43	1.88	1500	0.00545	0.660	45.2800	3.60912
18	10	29.43	3.76	2000	0.00572	0.756	44.8597	2.42956
19	15	9.81	0.94	2000	0.00269	0.336	51.4211	9.47321
20	15	9.81	1.88	1000	0.00215	0.432	53.3715	7.29033
21	15	9.81	3.76	1500	0.00251	0.492	52.0238	6.16070
22	15	19.62	0.94	1000	0.00323	0.408	49.8294	7.78680
23	15	19.62	1.88	1500	0.00359	0.504	48.9102	5.95139
24	15	19.62	3.76	2000	0.00404	0.588	47.8831	4.61245
25	15	29.43	0.94	1500	0.00503	0.444	45.9773	7.05234
26	15	29.43	1.88	2000	0.00539	0.576	45.3763	4.79155
27	15	29.43	3.76	1000	0.00431	0.672	47.3205	3.45261

WR: wear rate; COF: co-efficient of friction; S/N: signal-to-noise.

secondly by applied load, sliding distance, and sliding velocity. The WR of the produced composites decreases with increasing the wt.% of ZrO_2 content for this investigation. Here, the inclusions of ZrO_2 particles transfer from the composite to the tribo-layer due to surface deformation during sliding. This result in squeezing out of these particles reduces the WR. By considering applied load, the WR increases with an increase in load due to formation of severe plastic deformation. At high load condition, the higher WR has been observed due to temperature rise of the pin surface which removes a greater amount of metal. Similar reports have also been revealed by Baradeswaran et al. during wear process of AMCs.³²

The mean S/N ratio value for the WR was depicted in Table 6. The maximal value of the S/N ratio in the table is equivalent to the optimum level of the control parameters. Based on the S/N ratio result (Figure 3 & Table 6), the reinforcement at level A_3 (15 wt.% ZrO_2), applied load at level B_1 (9.81 N), sliding velocity at level C_1 (0.94 m/s) and sliding distance at level D_1 (1000 m) gives minimum WR. It is also computed the influence of control parameters on WR by delta value. The largest delta value indicates the most noteworthy parameter which is denoted as rank 1, subsequently by other parameters like rank 2 and 3 etc.. From Table 6, it can be found that reinforcement content was the most noteworthy factor on the WR, after that applied load

and sliding distance. The sliding velocity was insignificant factor which is not affects more on the WR. ANOVA is a statistical technique which is ensures the significant of parameters on the responses and also determined the percentage contribution of those parameters.³³ Table 6 depict the result of ANOVA for WR. From the table, F-ratio and P-value were used to reveal the impact of parameters at confidence level of 95% and significant level of 5%. The F-ratio of reinforcement ($F = 15.68$) and applied load ($F = 11.80$) are very greater than the tabulated F-value ($F_{0.05,2,18} = 3.55$), and also the P-value of the both parameters are less than 0.05, which are ensured the more influential factors on WR. Also, it is found that the percentage contribution of reinforcement is 50.92%, followed by applied load 36.65%. The sliding distance and sliding velocity are very less significant factors with contributions of 3.26% and 0.62%. The similar observations was reported for the dry sliding wear process of AA6351-SiC- B_4C composites.³⁴

The contour plots for WR is shown in Figure 4(a-c), it can be reveal that the interaction affect of parameters on WR of the tested composites. Figure 4(a) demonstrates the contour effect of WR with respect to reinforcement wt.% and applied load. It has been found that the less WR ($0.0024 \text{ mm}^3/\text{m}$) is achieved at low level of applied load with higher amount of reinforcement wt.%. An increase in applied load increasing the WR gradually

Table 3. Normalized decision and weight matrix.

Ex. No	Normalized decision matrix (r_{ij})		Normalized weight matrix (v_{ij})	
	WR	COF	WR	COF
1	0.170047	0.172942	0.085024	0.086471
2	0.198388	0.213418	0.099194	0.106709
3	0.223259	0.264932	0.111630	0.132466
4	0.183928	0.180301	0.091964	0.090151
5	0.212270	0.228136	0.106135	0.114068
6	0.255071	0.279651	0.127535	0.139825
7	0.297293	0.195020	0.148647	0.097510
8	0.275893	0.242855	0.137946	0.121427
9	0.268952	0.287010	0.134476	0.143505
10	0.153852	0.117748	0.076926	0.058874
11	0.178723	0.150864	0.089361	0.075432
12	0.146911	0.176622	0.073456	0.088311
13	0.189134	0.154544	0.094567	0.077272
14	0.182193	0.195020	0.091097	0.097510
15	0.167733	0.220777	0.083867	0.110388
16	0.200702	0.154544	0.100351	0.077272
17	0.209956	0.202379	0.104978	0.101189
18	0.220367	0.231816	0.110184	0.115908
19	0.103532	0.103029	0.051766	0.051515
20	0.082710	0.132466	0.041355	0.066233
21	0.096591	0.150864	0.048296	0.075432
22	0.124354	0.125107	0.062177	0.062553
23	0.138236	0.154544	0.069118	0.077272
24	0.155587	0.180301	0.077794	0.090151
25	0.193761	0.136146	0.096881	0.068073
26	0.207642	0.176622	0.103821	0.088311
27	0.165998	0.206058	0.082999	0.103029

due to high pressure creates at the interface of the contacting surfaces. However, the WR reduces when the inclusion of ZrO₂ particles into matrix alloy. The high wt.% of ZrO₂ particles addition enhancing the surface hardness which improves the wear resistance of fabricated composites. Figure 4(b) display the effect of sliding velocity with wt.% of reinforcement content on WR. It clearly understood that the minimum WR is produced by 15 wt.% inclusion of ZrO₂ particulates composite. It is also noted that the WR doesn't depend on sliding velocity because it was insignificant parameter reported in Table 6. The influence of reinforcement wt.% with sliding distance on WR is shown in Figure 4(c). It can be noticed that the less WR is obtained at middle level of sliding distance with 15 wt.% of ZrO₂ filled composite. The WR is increased with increase in sliding distance due to more removal of metal from the pin surface thus produces more WR of tested composite samples.

Effect of control parameters on COF

Figure 5 graphically illustrate the effect of various control parameters on the COF during dry sliding wear for the produced composites. From the graph, it can be observed that reinforcement has a predominant factor on COF, followed by sliding velocity, applied load, and sliding distance. The COF gradually reduces with an increasing

Table 4. Positive and negative ideal solutions.

Response	V_j^+	V_j^-
WR	0.04135	0.14865
COF	0.05151	0.14351

the wt.% of reinforcement content in the Al matrix. The 15 wt.% of ZrO₂ particles filled AA8011 matrix composite indicates the minimum value of COF which is 0.336 at 9.81 N applied load with 0.94 m/s sliding velocity. In common, the COF increases with increasing the applied load due to more contact pressure occur at the interface. Thus result in improving the value of COF owing to the formation of mechanically mixed layer (MML) and its fragmentation at the rubbing surface. With an increase in sliding velocity increase the COF due to more content of plastic deformation occur on pin surface. Furthermore, reduce in COF at middle level of sliding distance which ensure that these parameter is insignificant among the others. Hence, the change in COF value doesn't depend on the sliding distance. Similar observations were also reported by Ashiwani Kumar et al.³⁵ during wear process of Al-7075 alloy composites.

Table 7 depicts the mean S/N ratio of COF. The optimum level of each parameter is obtained from the mean S/N ratio value. Based on the S/N ratio (Figure 5 & Table 7) result, the minimum COF is obtained at level A₃ for reinforcement (15 wt.%), applied load at level B₁ (9.81 N), sliding velocity at level C₁ (0.94 m/s) and sliding distance at level D₂ (1500 m). It also noted that the factor of reinforcement was more important for getting low COF, later on sliding velocity and applied load. The sliding distance was less significant factor which is not influencing the COF. These observations are ensured by ANOVA result is shown in Table 7. From the table, The F-ratio of reinforcement (F = 112.80), sliding velocity (F = 97.13) applied load (F = 28.39) are very larger than the tabulated F-value (F_{0.05,2,18} = 3.55), and also the P-value is less than 0.05, which confirmed that those parameters are more significance on COF. The contribution of reinforcement is 45.58%, trailed by sliding velocity 39.25% and applied load 11.48%. The sliding distance is insignificant parameter with contribution of 0.05% only.

Figure 6(a)–(c) illustrates the contour graphs for COF with respect to control parameters. The combined effect of reinforcement wt.% with applied load on COF is shown in Figure 6(a). It clearly explore that the lower applied load (9.81 N) with higher ZrO₂ content of 15 wt.% provide the minimum COF (0.40 to 0.48). Because, the minimum load conditions creates less friction between the contacting surfaces thus produce low COF. And, also the incorporation of ZrO₂ particles tailored the properties of matrix alloy that will achieve the less frictional force. In Figure 6(b) show the response of COF with respect to parameters like wt.% of reinforcement and sliding velocity. It can be observed that the COF steadily increasing with increase in sliding velocity at maximum level. However, the addition of ZrO₂ content reduces the

COF at medium level of sliding velocity (1.88 m/s). Therefore, the COF chiefly controlled by sliding velocity reported in Table 7. The influence of reinforcement content with sliding distance on COF is shown in Figure 6(c). It has been reveal that the low COF value

attained at 15 wt.% of ZrO₂ content at a sliding distance from 1000 m to 2000 m. Hence, the sliding distance is insignificant parameter among the others.

Table 5. Separation measures and relative closeness value.

Ex. No	Separation measures		Relative closeness (RC_i^+)
	S_i^+	S_i^-	
1	0.05594	0.08545	0.60434
2	0.07996	0.06165	0.43535
3	0.10721	0.03863	0.26490
4	0.06368	0.07785	0.55007
5	0.09006	0.05171	0.36477
6	0.12340	0.02143	0.14799
7	0.11674	0.04600	0.28266
8	0.11924	0.02454	0.17067
9	0.13090	0.01417	0.09770
10	0.03633	0.11094	0.75331
11	0.05364	0.09028	0.62728
12	0.04884	0.09328	0.65636
13	0.05912	0.08551	0.59122
14	0.06775	0.07368	0.52094
15	0.07262	0.07276	0.50046
16	0.06438	0.08198	0.56012
17	0.08073	0.06081	0.42966
18	0.09426	0.04734	0.33434
19	0.01042	0.13360	0.92768
20	0.01472	0.13223	0.89981
21	0.02491	0.12127	0.82959
22	0.02357	0.11845	0.83402
23	0.03788	0.10350	0.73209
24	0.05312	0.08870	0.62546
25	0.05795	0.09149	0.61223
26	0.07250	0.07111	0.49514
27	0.06625	0.07713	0.53794

Effect of control parameters on Rc

The main effect of control parameters with RC value is shown in Figure 7. It clearly noticed the optimal level of parameters for obtain the low WR and COF of the fabricated AA8011-ZrO₂ composites. Based on the plot (Figure 7), the optimum level of control parameters are A₃B₁C₁D₂, which reveal that reinforcement at level 3 (15 wt.%), applied load at level 1 (9.81 N), sliding velocity at level 1 (0.94 m/s) and sliding distance at level 2 (1500 m).

Table 8 depicts the response of mean RC with each level of parameters. The highest value of delta indicates that the reinforcement (rank 1) was the primary notable parameter on the RC trailed by applied load (rank 2) and sliding velocity (rank 3). The sliding distance (rank 4) indicates the less significant parameter on RC. This observation can be confirmed by ANOVA. Table 8 shows the ANOVA results for RC value. From the table, F-ratio of reinforcement (F = 103.93), applied load (F = 26.32) and sliding velocity (F = 12.84) are higher than the tabulated F-value ($F_{0.05,2,18} = 3.55$) and also the P-value of those parameters are less than 0.05, which confirms the significance on RC. The contribution of parameters on RC is shown in Figure 8. It reveals that the reinforcement was the more important parameter with a contribution of 55.06%, subsequently by applied load 26.32% and sliding velocity 12.84%. The sliding distance was less significant with contribution is 1.02% only. The R-Sq (95.23%) and adj R-Sq (93.11%) values are very close to one which ensured that the model was predicted with high accuracy.

Table 6. S/N ratio and ANOVA for WR.

Mean of S/N ratio					
Level	A	B	C	D	Optimum level
1	44.57	48.61*	46.99*	47.19*	A ₃ B ₁ C ₁ D ₁ (* optimum level of parameter)
2	46.53	46.86	46.67	46.97	
3	49.12*	44.75	46.57	46.07	
Delta	4.55	3.86	0.41	1.12	
Rank	1	2	4	3	

ANOVA						
Control parameters	DoF	Adj.SS	Adj.MS	F-ratio	P-value	Contribution (%)
Reinforcement	2	0.0000250	0.0000125	53.83	0.000	50.92
Applied load	2	0.0000180	0.0000090	38.83	0.000	36.65
Sliding velocity	2	0.0000003	0.0000002	0.65	0.535	0.62
Sliding distance	2	0.0000016	0.0000008	3.49	0.052	3.26
Residual error	18	0.0000042	0.0000002	--	--	8.55
Total	26	0.0000491	--	--	--	100

S = 0.000481502; R-Sq = 91.49%; R-Sq(adj) = 87.71%

DOF: degrees of freedom; Adj.SS: adjusted sum of square; Adj.MS: adjusted mean square.

Table 7. S/N ratio and ANOVA for COF.

Mean of S/N ratio					
Level	A	B	C	D	Optimum level
1	2.656	5.731*	6.450*	4.556	A ₃ B ₁ C ₁ D ₂ (* optimum level of parameter)
2	4.888	4.341	4.386	4.697*	
3	6.286*	3.757	2.994	4.576	
Delta	3.630	1.974	3.456	0.141	
Rank	1	3	2	4	

ANOVA						
Control parameters	DoF	Adj.SS	Adj.MS	F-ratio	P-value	Contribution (%)
Reinforcement	2	0.298400	0.149200	112.80	0.000	45.58
Applied load	2	0.075104	0.037552	28.39	0.000	11.48
Sliding velocity	2	0.256928	0.128464	97.13	0.000	39.25
Sliding distance	2	0.000384	0.000192	0.15	0.866	0.05
Residual error	18	0.023808		--	--	3.64
Total	26	0.654624	--	--	--	100

S = 0.0363685; R-Sq = 96.36%; R-Sq(adj) = 94.75%

Table 8. Mean and ANOVA for RC.

Mean of RC					
Level	A	B	C	D	Optimum level
1	0.3243	0.6665*	0.6351*	0.5480	A ₃ B ₁ C ₁ D ₂ (* optimum level of parameter)
2	0.5526	0.5408	0.5195	0.5489*	
3	0.7216*	0.3912	0.4439	0.5015	
Delta	0.3973	0.2753	0.1912	0.0474	
Rank	1	2	3	4	

ANOVA						
Control parameters	DoF	Adj.SS	Adj.MS	F-ratio	P-value	Contribution (%)
Reinforcement	2	0.71554	0.35777	103.93	0.000	55.06
Applied load	2	0.34203	0.17102	49.68	0.000	26.32
Sliding velocity	2	0.16691	0.08346	24.24	0.000	12.84
Sliding distance	2	0.01325	0.00662	1.92	0.175	1.02
Residual error	18	0.06196	0.00344	--	--	4.76
Total	26	1.29970	--	--	--	100

S = 0.0586717; R-Sq = 95.23%; R-Sq(adj) = 93.11%

RC: relative closeness.

Table 9. Confirmation experimental results.

Method	Response	Optimal level	Predicted	Experimental	Error (%)
Taguchi method	WR (g/min)	A ₃ B ₁ C ₁ D ₁	0.00241	0.00258	6.5
	COF	A ₃ B ₁ C ₁ D ₂	0.296	0.316	6.3
TOPSIS method	RC	A ₃ B ₁ C ₁ D ₂	0.97367	0.92768	4.7

WR: wear rate; COF: co-efficient of friction; RC: relative closeness.

Confirmation experiments

The confirmation experiment was carried out by the determined optimal level of control parameters to verify the output responses during dry sliding wear process of AA8011-wt.% ZrO₂ composite. The predicted result of

the output responses are calculated by using equation (9).³¹

$$\eta_{pre} = \eta_m + \sum_{k=1}^n (\eta_i - \eta_m) \quad (9)$$

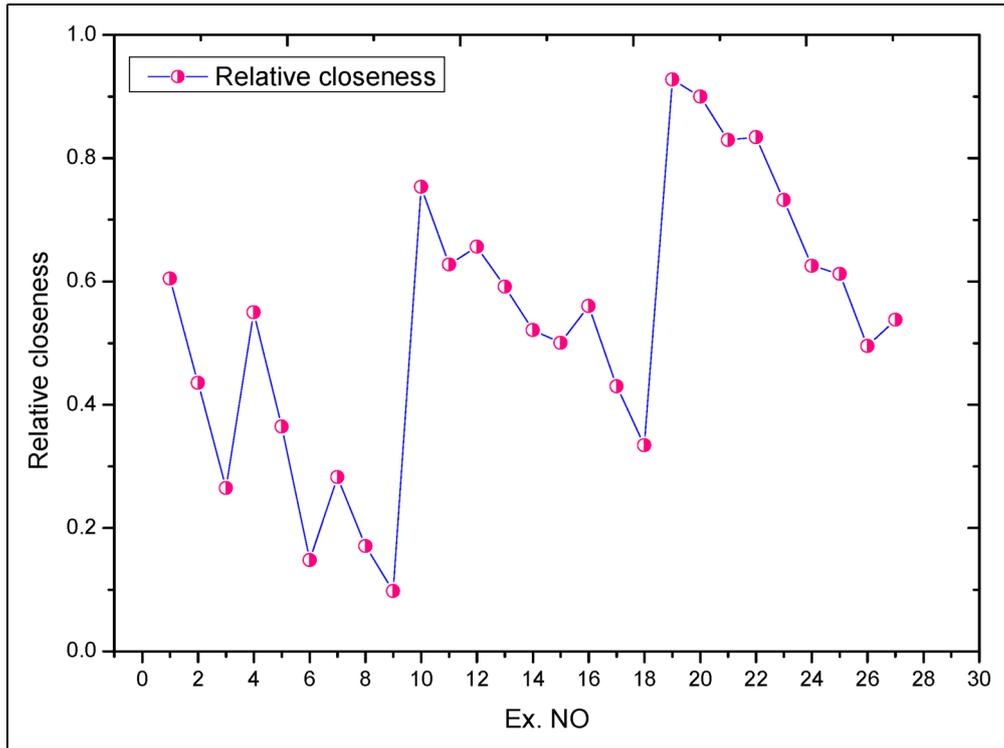


Figure 2. Rank plot for RC.

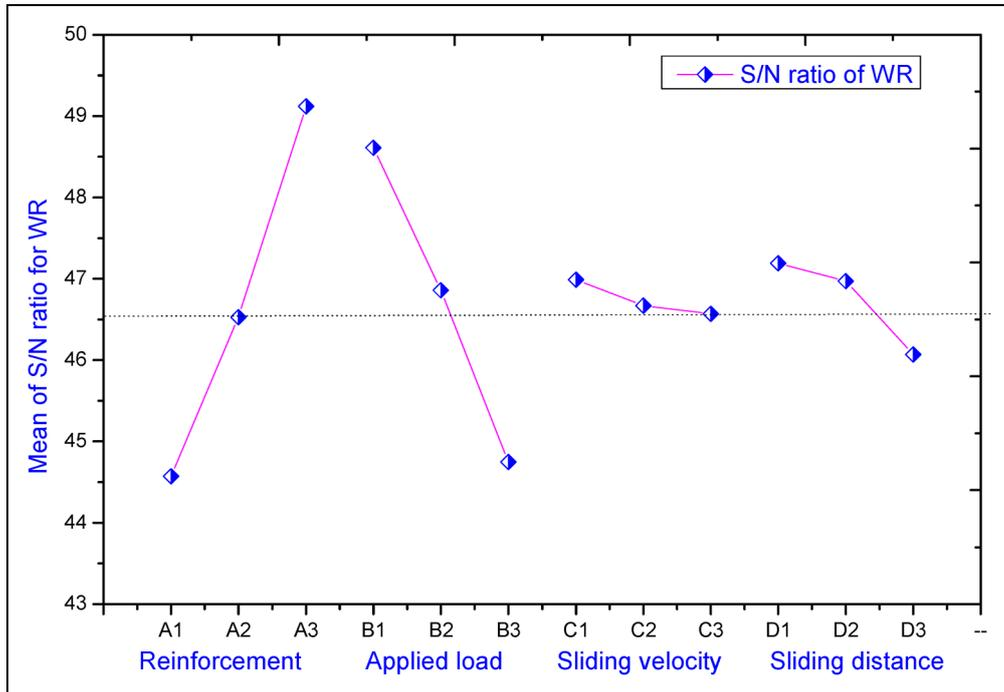


Figure 3. Main effect plot for WR.

where, η_{pre} predicted value of response, η_m total mean value of response, η_i is response mean value at the optimum level and k number of control parameters. Table 9 shows the predicted and experimental result of the output responses at the optimal range of control parameters obtained by Taguchi and TOPSIS method. It

clearly observed that a very low percentage error of 6.5%, 6.3% and 4.7% were obtained between the predicted and experimental result thus showing a very good correlation. Hence, the present analysis performed are accurate and can be used as predictive tools for wear applications.

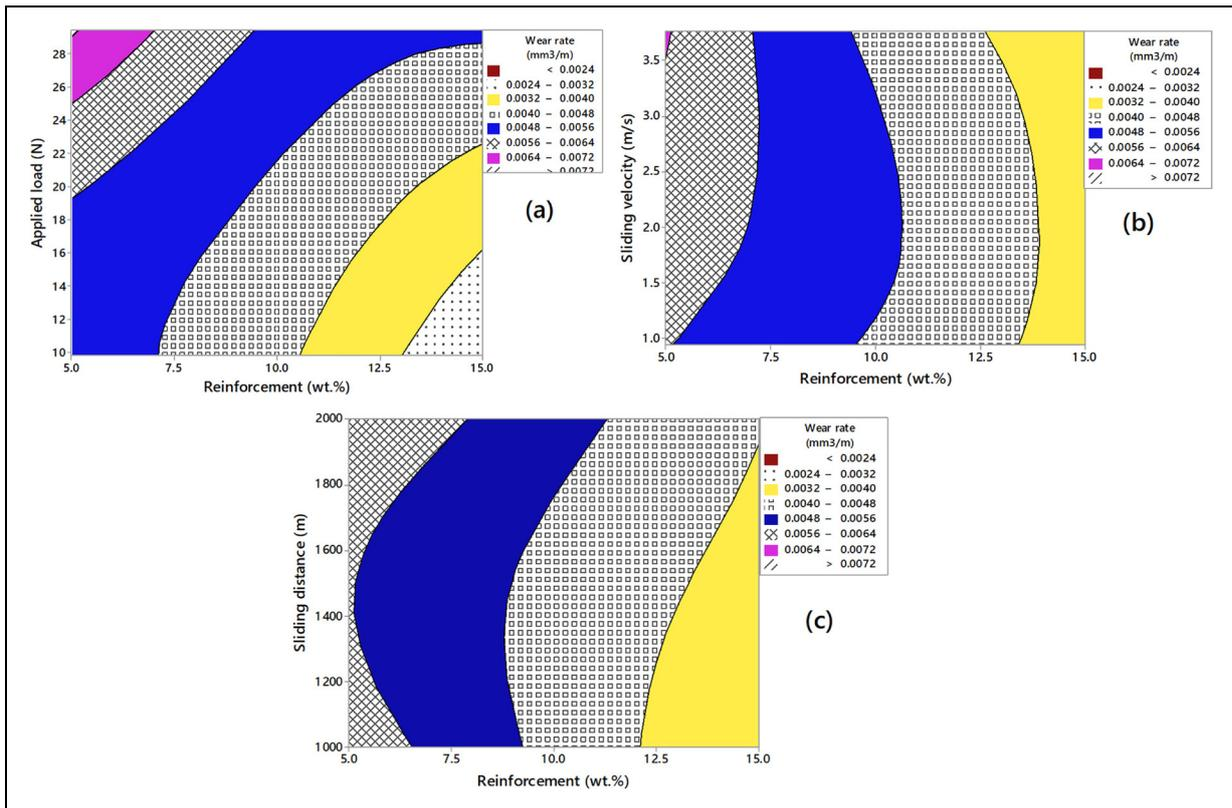


Figure 4. Contour plot for WR (a) reinforcement vs. applied load, (b) reinforcement vs. sliding velocity and (c) reinforcement vs. sliding distance.

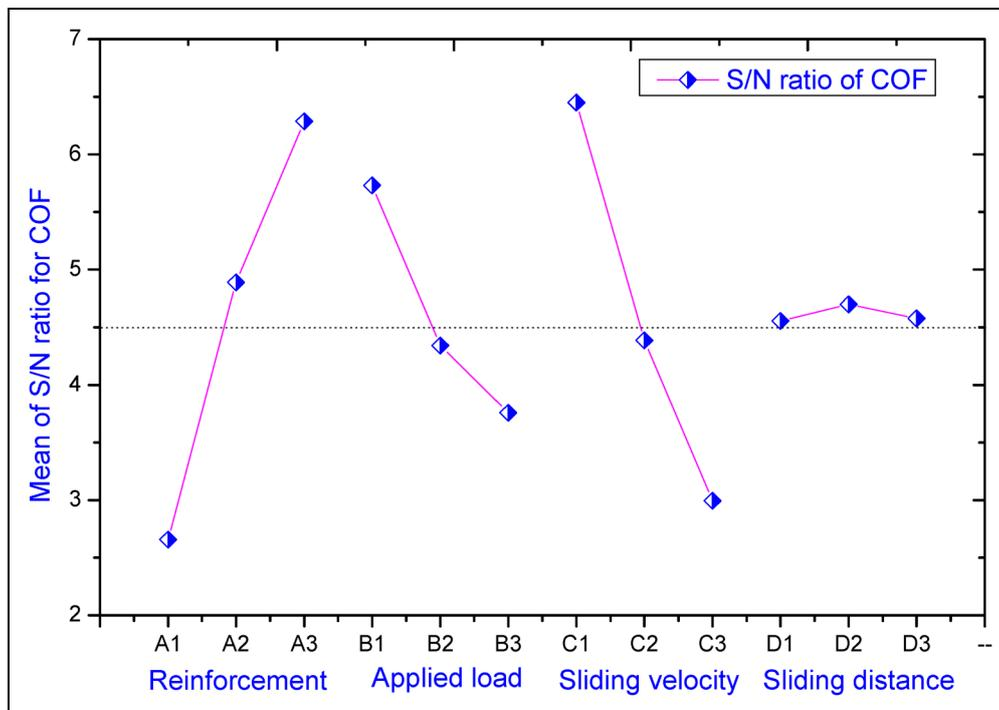


Figure 5. Main effect plot for COF.

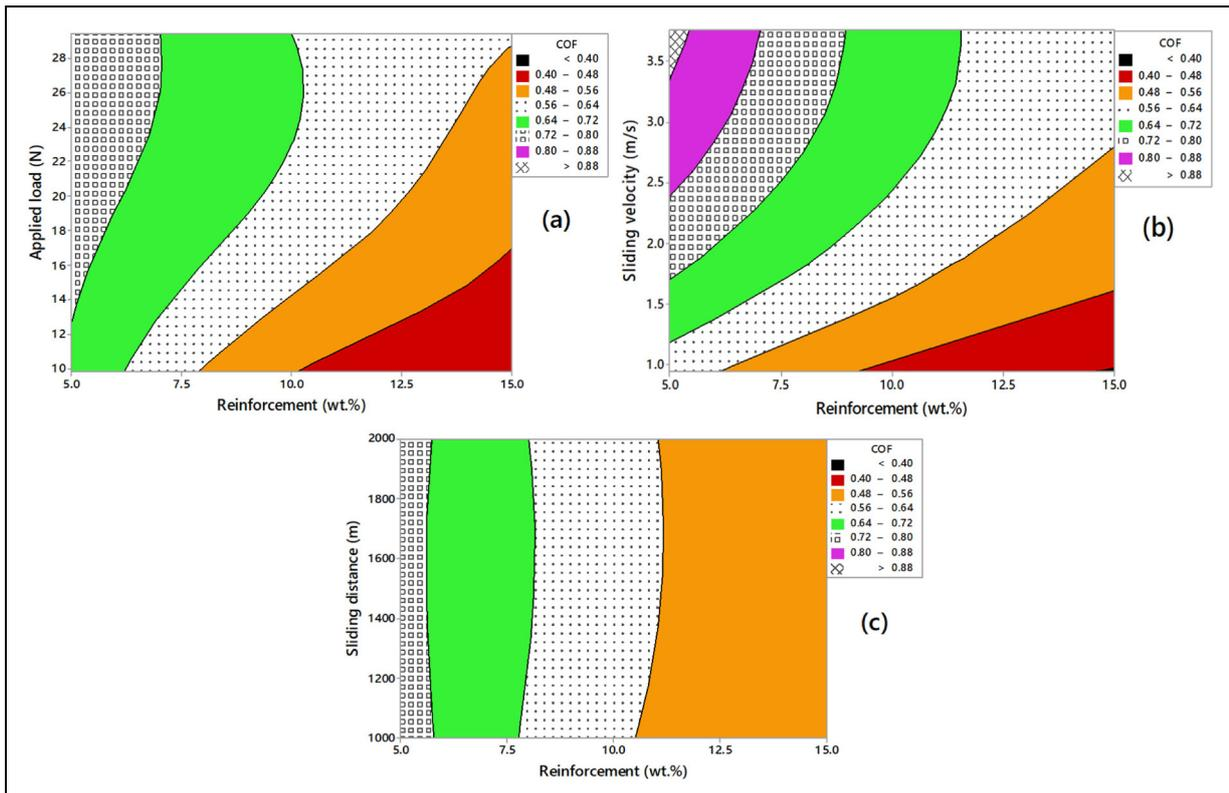


Figure 6. Contour plot for COF (a) reinforcement vs. applied load, (b) reinforcement vs. sliding velocity and (c) reinforcement vs. sliding distance.

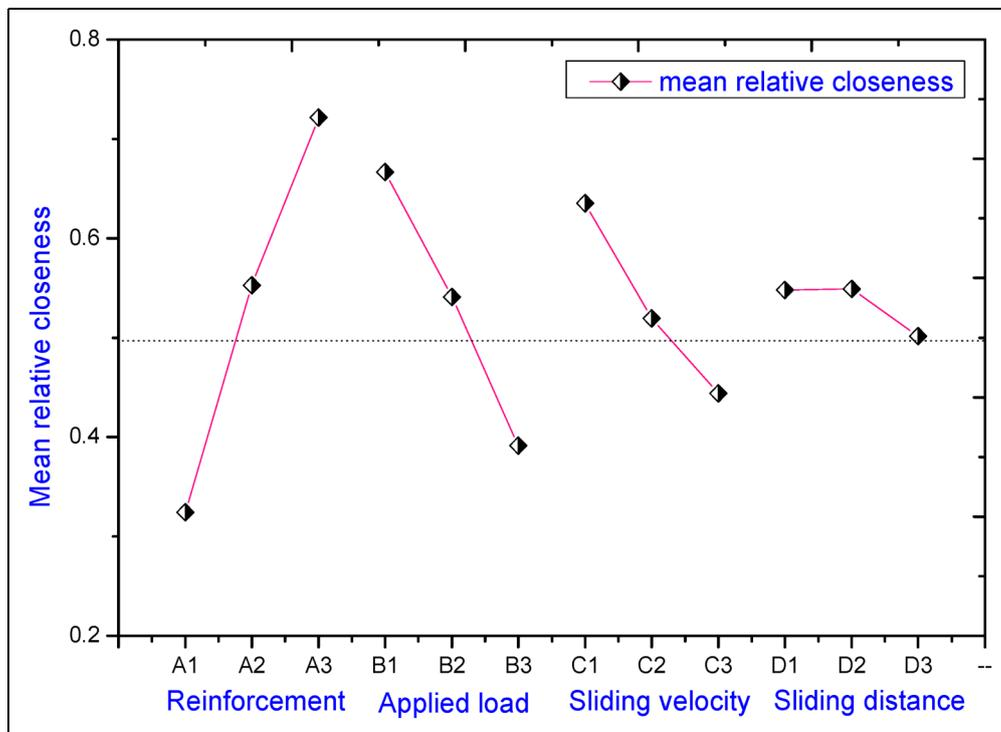


Figure 7. Main effect plot for RC.

Worn surface morphology

The SEM morphology of the worn surfaces of AA8011-5 wt.% ZrO₂, AA8011-10 wt.% ZrO₂ and AA8011-15 wt.% ZrO₂ composite specimens tested at various conditions of control parameters are shown in

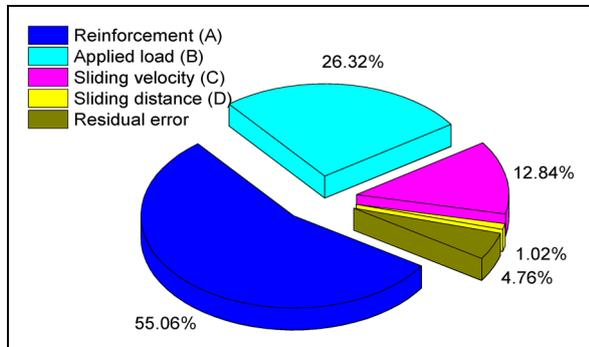


Figure 8. Contribution of parameters on RC.

Figure 9(a-d). For the worn surfaces of 5 wt.% ZrO₂ filled AA8011 matrix composite at parametric conditions of 29.43 N load, 0.94 sliding velocity and 2000 m sliding distance is display in Figure 9(a). It has been reveal that the continuous grooves and delamination are formed over the worn surface of the specimen along the sliding direction. This resulting in more removal of material due to formation of more heat at the interface of the contacting surfaces. However, the inclusion of ZrO₂ particles produce the MML layer at the specimen surface, thus reduce the WR because it act as a solid lubricant. In Figure 9(b) explore the worn surface of (AA8011-10 wt.% ZrO₂) composite at a load of 29.43 N, sliding velocity of 0.94 m/s and sliding distance of 2000 m, respectively. It can be seen to have the ploughs with macro cracks at a few regions, resulting in more WR. This was happened due to the dislodgement of ZrO₂ particles along the sliding direction which act as a abrasive material. The worn surface of the composite specimen (Figure 9(c)) reveal that the fine grooves are creates

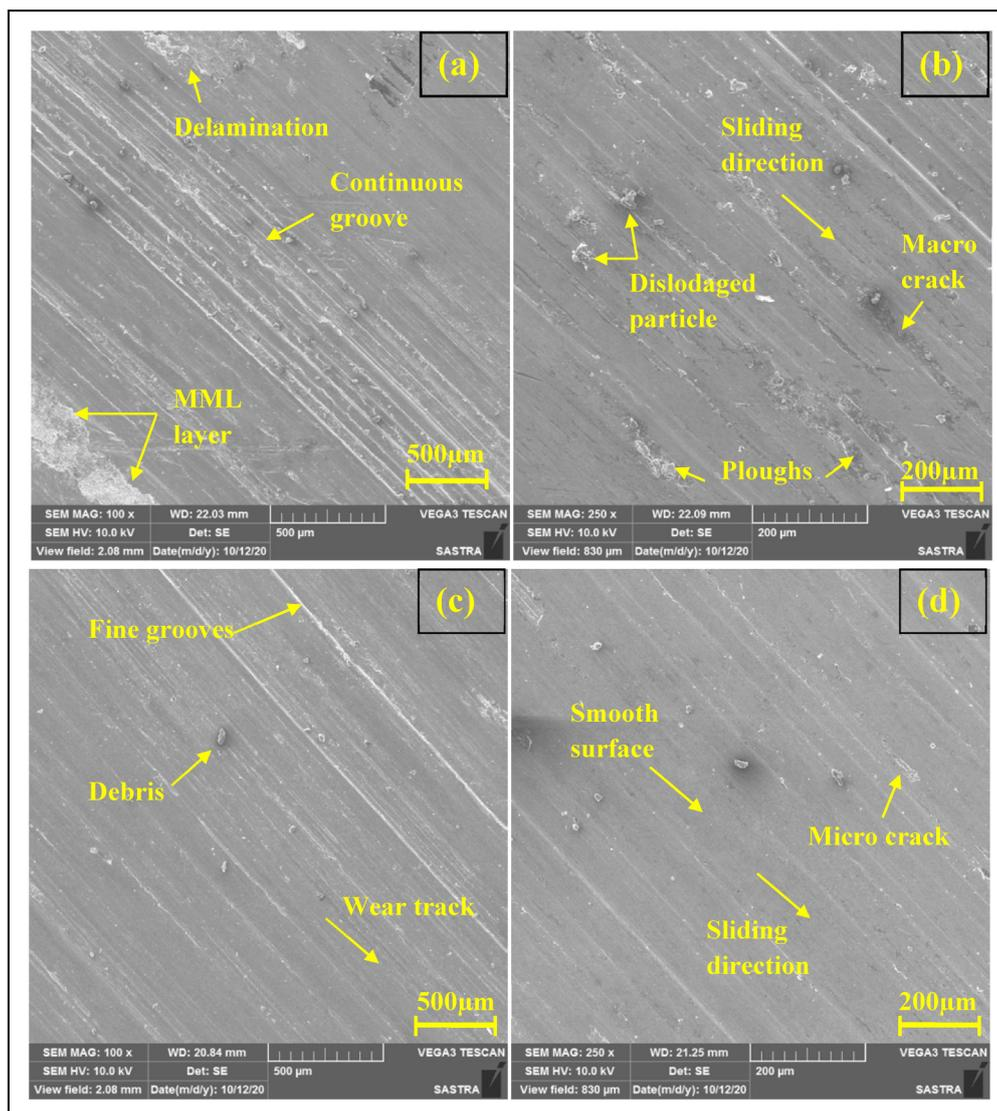


Figure 9. Worn surfaces (a) 5 wt.% ZrO₂; (b) 10 wt.% ZrO₂ (c) 15 wt.% ZrO₂ and (d) at optimal condition.

at few region which resulting in a less WR. The reason for that, the inclusion of reinforcement particles act as the load bearing elements which protect the load transfer to the matrix. Figure 9(d) illustrate the worn surface of optimal parametric conditions on 15 wt.% ZrO₂ composit with a load of 9.81 N, sliding velocity of 0.94 m/s and sliding distance of 1500 m, respectively. It clearly found that the smooth surface and micro crack are visible at some areas over the worn surface of the specimen. Because, the lower load at minimum sliding velocity on the higher amount of ZrO₂ (15 wt.%) particles reinforced composite enhance the wear resistance.

Conclusions

The effect of control factors for the dry sliding wear behaviour of AA8011 matrix composites reinforced with ZrO₂ particles were studied in the present work. The following key points were concluded from this study;

- Stir casting method was effectively used to fabricated the AA8011 matrix based composites incorporated with various proportions (5 wt.%, 10 wt.% and 15 wt.%) of ZrO₂ particulates.
- The combination of Taguchi and TOPSIS method was employed to determine the optimum level of control factors for dry sliding wear behaviour of produced composites.
- As a result of the Taguchi method, the optimum level of control factors for minimum wear rate: reinforcement: 12 wt.%, applied load: 9.81 N, sliding velocity: 0.94 m/s and sliding distance: 1000 m, while the optimum level for minimum COF: reinforcement: 12 wt.%, applied load: 9.81 N, sliding velocity: 0.94 m/s and sliding distance: 1500 m.
- The optimum level of control factors combinations were obtained by the response of relative closeness values: reinforcement: 12 wt.%, applied load: 9.81 N, sliding velocity: 0.94 m/s and sliding distance: 1500 m.
- As a result of ANOVA reveals that, reinforcement and applied load were the most noteworthy factors for the multiple responses and they contribute 55.06% and 26.32% respectively.
- Worn surface morphology revealed that the applied load play an vital role in proceuce the WR and also found that the formation of MML layer protect the fabricated composite specimen from the WR.
- In this study ensured that the proposed combination of Taguchi and TOPSIS approach was more efficient method for solving the multi-response optimization problems.

Declaration of conflicting interests

The author(s) declared no potential conflicts of interest with respect to the research, authorship, and/or publication of this article.

Funding

The author(s) received no financial support for the research, authorship, and/or publication of this article.

ORCID iD

Alagarsamy S.V.  <https://orcid.org/0000-0002-6564-0346>

References

1. Alagarsamy SV, Ravichandran M, Raveendran P, et al. Evaluation of micro hardness and optimization of dry sliding wear parameters on AA7075 (al-zn-mg-cu) matrix composites. *J Balk Tribol Assoc* 2019; 25: 730–739.
2. Idusuyi N and Olayinka I J. Dry sliding wear characteristics of aluminium metal matrix composites: a brief overview. *J Mater Res Technol* 2019; 8: 3338–3346.
3. Kaushik N and Singhal S. Dry-sliding wear analysis of SiC reinforced AA6063 as-cast aluminum metal matrix composites. *Mater Today: Proceed* 2018; 5: 24147–24156.
4. Baskaran S, Anandkrishnan V and Duraiselvam M. Investigations on dry sliding wear behavior of in situ casted AA7075–TiC metal matrix composites by using taguchi technique. *Mater Des* 2014; 60: 184–192.
5. Sakthivelu S, Sethusundaram PP, Ravichandran M, et al. Experimental investigation and analysis of properties and dry sliding wear behavior of al-fe-si alloy matrix composites. *Silicon* 2020; 13: 1285–1294.
6. Alagarsamy SV and Ravichandran M. Synthesis, microstructure and properties of TiO₂ reinforced AA7075 matrix composites via stir casting route. *Mater Res Express* 2019; 6: 1–15.
7. Suresh R. Comparative study on dry sliding wear behavior of mono (Al2219/B₄C) and hybrid (Al2219/B₄C/Gr) metal matrix composites using statistical technique. *J Mech Beha Mater* 2020; 29: 57–68.
8. Radhika N and Venkata Priyanka ML. Investigation of adhesive wear behaviour of zirconia reinforced aluminium metal matrix composite. *J Eng Sci Technol* 2017; 12: 1685–1696.
9. Haq MIU and Anand A. Dry sliding friction and wear behavior of AA7075-Si₃N₄ composite. *Silicon*. 2018; 10: 1819–1829.
10. Jha AK, Prarsd SV and Upadhyaya GS. Dry sliding wear of sintered 6061 aluminium alloy-graphite particles composites. *Tribol Int* 1989; 22: 321–327.
11. Yigezu BS, Jha PK and Mahapatra MM. The key attributes of synthesizing ceramic particulate reinforced Al-based matrix composites through stir casting process: a review. *Mater Manuf Process* 2013; 28: 969–979.
12. Saravanan V, Thyla PR and Balakrishnan SR. The dry sliding wear of cenosphere -aluminium metal matrix composite. *Adv Compos Lett* 2014; 23: 1–10.
13. Karthikeyan G and Jinu G. Mechanical properties and metallurgical characterization of LM25/ZrO₂ fabricated by stir casting method. *Rev Mater* 2019; 24: 1–14.
14. Dong B-X, Li Q, Wang Z-F, et al. Enhancing strength-ductility synergy and mechanisms of Al-based composites by size-tunable in-situ TiB₂ particles with specific spatial distribution. *Compos. B. Eng* 2021; 217: 108912. (1–15).
15. Madhusudhan M, Naveen GJ and Mahesha K. Mechanical characterization of AA7068-ZrO₂ reinforced metal matrix composites. *Mater Today: Proceed* 2017; 4: 3122–3130.

16. Yang H-Y, Wang Z, Chen L-Y, et al. Interface formation and bonding control in high-volume-fraction (TiC + TiB₂)/Al composites and their roles in enhancing properties. *Compos. B. Eng* 2021; 209: 108605. (1–11).
17. Zhu H, Sun X, Huang J, et al. Dry sliding tribological behavior at elevated temperature of in situ aluminum matrix composites fabricated by al-ZrO₂-C system with different mole ratio of C/ ZrO₂. *Powder Metall Min* 2017; 6: 1000153. (1–5).
18. Pandiyarajan P, Maran S, Marimuthu S, et al. Mechanical and tribological behavior of the metal matrix composite AA6061/ZrO₂/C. *J Mech Sci Technol* 2017; 31: 4711–4717.
19. Alagarsamy SV and Ravichandran M. Investigations on tribological behaviour of AA7075-TiO₂ composites under dry sliding conditions. *Ind Lubr Tribol* 2019; 71: 1064–1071.
20. Alagarsamy SV and Ravichandran M. Parametric studies on dry sliding wear behaviour of A1–7075 alloy matrix composite using S/N ratio and ANOVA analysis. *Mater Res Express* 2020; 7: 1–17.
21. Kumar N and Manoj MK. Influence of B₄C on dry sliding wear behavior of B₄C /Al–Mg–Si composites synthesized via powder metallurgy route. *Met Mater Int* 2020; 27: 4120–4131.
22. Ayyanar S, Gnanavelbabu A, Rajkumar K, et al. Studies on high temperature wear and friction behaviour of AA6061/B₄C/hBN hybrid composites. *Met Mater Int* 2021; 27: 3040–3057.
23. Ghandvar H, Farahany S, Idris MH, et al. Dry sliding wear behavior of A356-ZrO₂ metal matrix composite. *Adv Mater Res* 2015; 1125: 116–120.
24. Aruchamy S, Soundararajan R, Sathish Kumar K, et al. Design and couple field analysis of uncoated and coated aluminium metal matrix hybrid composite piston. *SAE Tech Pap* 2020; 2020–28–0391: 1–8.
25. Kumar M. Mechanical and sliding wear performance of AA356-Al₂O₃/SiC/graphite alloy composite materials: parametric and ranking optimization using taguchi DOE and hybrid AHP-GRA method. *Silicon* 2020; 13: 2461–2477.
26. Magibalan S, Senthilkumar P, Senthilkumar C, et al. Optimization of wear parameters for aluminium 4% fly-ash composites. *J Eng Mater Sci* 2020; 27: 458–464.
27. Ajith, Sakthivel M, Manoj K, et al. Dry sliding behaviour of aluminium 5059/SiC/MoS₂ hybrid metal matrix composites. *Mater Res* 2017; 20: 1697–1706.
28. Dharmalingam S, Subramanian R and Kok M. Optimization of abrasive wear performance in aluminium hybrid metal matrix composites using taguchi-grey relational analysis. *Proc IMech Part J: J Eng Tribol* 2013; 227: 749–760.
29. Kosal S, Ficici F, Kayikci R, et al. Experimental optimization of dry sliding wear behaviour of in situ AlB₂/Al composite based on Taguchi's Method. *Mater Des* 2012; 42: 124–130.
30. Kumar H and Harsha AP. Taguchi optimization of various parameters for tribological performance of polyalphaolefins based nanolubricants. *Proc IMech Part J: J Eng Tribol* 2020; 235: 1262–1280.
31. Alagarsamy SV, Raveendran P and Ravichandran M. Investigation of material removal rate and tool wear rate in spark erosion machining of al-fe-si alloy composite using taguchi coupled TOPSIS approach. *Silicon* 2021; 13: 2529–2543.
32. Baradeswaran SC, Vettivel SC, Elaya Perumal A, et al. Experimental investigation on mechanical behaviour, modelling and optimization of wear parameters of B₄C and graphite reinforced aluminium hybrid composites. *Mater Des* 2014; 63: 620–632.
33. Vijayakumar S and Karunamoorthy L. Modelling and analysis on wear behaviour of aluminium metal matrix composites: a statistical approach. *Tribol* 2011; 5: 65–71.
34. Thirumalai Kumaran S, Uthayakumar M and Aravindan S. Analysis of dry sliding friction and wear behaviour of AA6351-SiC-B₄C composites using grey relational analysis. *Tribol* 2014; 8: 187–193.
35. Kumar A, Patnaik A and Bhat IK. Investigation of nickel metal powder on tribological and mechanical properties of Al-7075 alloy composites for gear materials. *Powder Metall* 2017; 60: 371–383.